

Paleoclimatic and Diagenetic History of the Late Quaternary Sediments in a Core from the Southeastern Arabian Sea: Geochemical and Magnetic Signals

VENIGALLA PURNACHANDRA RAO¹*, PRATIMA MOHAN KESSARKAR¹, MELOTH THAMBAN²
and SHIVA KUMAR PATIL³

¹National Institute of Oceanography, Council of Scientific and Industrial Research,
Dona Paula - 403 004, Goa, India

²National Centre for Antarctic and Ocean Research, Headland Sada - 403 804, Goa, India

³Dr. K. S. Krishna Geomagnetic Research Laboratory, Indian Institute of Geomagnetism,
Allahabad - 221 505, Uttar Pradesh, India

(Received 15 April 2009; in revised form 25 September 2009; accepted 26 September 2009)

Geochemical and rock-magnetic investigations were carried out on a sediment core collected from the SE Arabian Sea at 1420 m depth in oxygenated waters below the present-day oxygen minimum zone. The top 250 cm of the core sediments represent the last 35 kaBP. The $\delta^{18}\text{O}$ values of *Globigerinoides ruber* are heaviest during the Last Glacial Maximum (LGM) and appear unaffected by low-saline waters transported from the Bay of Bengal by the strong northeast monsoon and West Indian coastal current. The signatures of Bølling-Allerød and Younger Dryas events are distinct in the records of magnetic susceptibility, organic carbon (OC) and $\delta^{18}\text{O}$. Glacial sediments show higher OC, CaCO_3 , Ba, Mo, U and Cd, while the early-to-late Holocene sediments show increasing concentrations of OC, CaCO_3 , Ba, Cu, Ni and Zn and decreasing concentrations of Mo, U and Cd. Productivity induced low-oxygenated bottom waters and reducing sedimentary conditions during glaciation, and productivity and oxygenated bottom waters in the Holocene are responsible for their variation. The core exhibits different stages of diagenesis at different sediment intervals. The occurrence of fine-grained, low-coercivity, ferrimagnetic mineral during glacial periods is indicative of its formation in organic-rich, anoxic sediments, which may be analogous to the diagenetic magnetic enhancement known in sapropels of the Mediterranean Sea and Japan Sea. The glacial sediments exhibiting reductive diagenesis with anoxic sedimentary environment in this core correspond to reductive diagenesis and intermittent bioturbation (oxygenation) reported in another core in the vicinity. This suggests that the poorly oxygenated bottom water conditions during glacial times should not be generalized, but are influenced locally by productivity, sedimentation rates and sediment reworking.

Keywords:

- Rock magnetic properties,
- redox-sensitive elements,
- sedimentary environment,
- diagenetic magnetic minerals,
- productivity,
- SE Arabian Sea,
- late Quaternary.

1. Introduction

Sediments in the Arabian Sea form an important archive for understanding climate and environmental conditions during the Quaternary. For more than two decades, numerous sedimentary records have been investigated from its northwestern and northeastern margins and the deep Arabian Sea (Van Campo *et al.*, 1982; Clemens and Prell, 1990; Shimmield *et al.*, 1990; Shimmield and

Mowbray 1991; Prell *et al.*, 1992; Sirocko *et al.*, 1996, 2000; Reichart *et al.*, 1997; Schulz *et al.*, 1998; von Rad *et al.*, 1999; Schnetger *et al.*, 2000). The records reveal the history of upwelling-related productivity driven by the monsoons. The past variations in productivity are related to climate change through glacial/interglacial cycles and are linked to such global parameters as ice volume, deep water circulation and continental climate. The southeastern Arabian Sea is affected by both southwest and northeast monsoons and a few sedimentary records report productivity and climate change (Sarkar *et al.*, 1990, 1993; Thamban *et al.*, 2001; Pattan *et al.*, 2003;

* Corresponding author. E-mail: vprao@nio.org

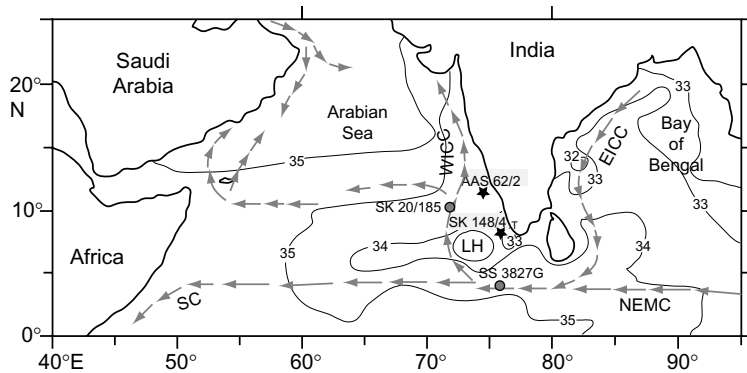


Fig. 1. Location of sediment cores: SK 148/4, SK 20/185, AAS 62/2 and SS 3827G. Base map and currents are adopted from Tiwari *et al.* (2005). Direction of the northeast monsoon currents (NEMC) and salinity contours (Nos. 32–35) for that period are also given. SC - Somali current, LH - Laccadive High, EICC - East India Coastal Current, WICC - West India Coastal Current. T - Thiruvananthapuram.

Banakar *et al.*, 2005; Singh *et al.*, 2006). As the strength of the monsoons varies significantly within the Arabian Sea during glacial/interglacial cycles (Duplessy, 1982), one would expect significant regional variations in productivity. The biological and geochemical proxies developed for productivity in one area may only be of limited use in other areas, as these proxies are affected by various other processes (bioturbation, diagenesis etc.), which may destroy or mask the primary geochemical signals (Schnetger *et al.*, 2000; Rao *et al.*, 2008). On the other hand, rock magnetic parameters (concentration, mineralogy and grain size) of the sediments respond to environmental change and have been used extensively to address provenance, climate-related and diagenetic changes (Bloemendal *et al.*, 1988; Karlin, 1990; Leslie *et al.*, 1990; Vigliotti *et al.*, 1999). It has been shown that the variations in magnetic susceptibility are related to global oxygen isotope fluctuations (Vigliotti, 1997). They respond to a global model of the atmospheric and oceanic circulation and are coincident with the Earth's orbital periods (Bloemendal *et al.*, 1988). The effect of diagenesis on magnetic minerals (dissolution of detrital magnetite and other iron-bearing phases and formation of new magnetic minerals by (bio-)authigenesis is well known: (Robinson *et al.*, 2002; Liu *et al.*, 2004; Rey *et al.*, 2005; Hayashida *et al.*, 2007). In this paper a multiproxy approach has been adopted to determine the past climate and diagenetic conditions. The objectives of the paper are to investigate sedimentological, geochemical and rock magnetic characteristics of the sediments in a core from the southeastern Arabian Sea and compare these results with other cores in the vicinity to better understand climate, oceanographic and diagenetic conditions during the late Quaternary.

A sediment core SK148/4 collected from the southwestern margin of India, off Thiruvananthapuram (Fig. 1) at 1420 m depth in oxygenated waters below the

present-day depths of the oxygen minimum zone (OMZ: 150–900 m) was investigated. The results of this core were compared with three other sediment cores located in the vicinity (see Fig. 1). Core AAS 62/2 is from 1380 m depth located to the north of the core SK 148/4, while cores SK 20/185 and SS 3827G are from 3564 m and 3118 m depths, located towards west and south, respectively. Strong seasonal winds during the southwest monsoon (SWM; June–September) and northeast monsoon (NEM; November–February) invoke large seasonal changes in hydrography and particle fluxes. During present times, the SWM is strong in the Arabian Sea and induces upwelling of cold, nutrient-rich sub-surface waters leading to enhanced productivity. The NEM is weak in the Arabian Sea and productivity occurs due to winter cooling, which drives convective mixing and injection of nutrients to the euphotic zone.

2. Materials and Methods

During the 148th cruise of *ORV Sagar Kanya* a 2.8 m long gravity core was recovered at 1420 m water depth from the southwestern margin of India (Fig. 1). The sediments throughout the length of the core are olive grey, clayey silt/silty clays. The core was sectioned onboard at 1 cm interval. Sub-samples were dried at <40°C. The organic carbon (OC) content of the 69 sediment intervals was determined using a CNS analyser (NCS 2500). The OC reproducibility was better than 1%. The CaCO_3 content of 88 sediment samples was measured using a coulometer with reproducibility of measurements better than 5%. Grain size analyses were performed on 175 samples free of carbonate and organic matter (1N HCl and H_2O_2 treated), using a Malvern Laser Particle size analyzer (Master-Sizer 2000) and a percentage of the clay (<4 μm) volume was used for the present study. Powdered samples were weighed accurately and treated with

Table 1. Accelerator Mass Spectrometer (AMS) ages of sediment intervals dated in the core SK 148/4.

Depth interval in the core (cm)	Lab. code at WHOI	Measured age (years)	Error age	Calibrated age (2σ) range (years)
17–20	47668	3070	45	2454–2879
51–54	47669	6280	35	6398–6743
70–73	47670	9350	50	9739–10209
97–100	47671	14050	65	15646–16512
148–154	47672	19500	70	22265–22665

WHOI - Woods Hole Oceanographic Institution, USA.

1N HCl, washed with distilled water to remove acid, dried and weighed again. The acid-insoluble residue (AIR) of the sample was calculated by subtracting this weight from the total weight. For the oxygen isotope analyses, monospecific, planktonic foraminifer *Globigerinoides ruber* (250–300 μm size fraction) was handpicked from the coarse fraction and repeatedly cleaned ultrasonically. About 10 *G. ruber* tests were selected from each of the 60 sediment intervals and analyzed for stable oxygen isotopes on a Micromass Optima IRMS system at the Geological Survey of Japan (GSJ), Tsukuba. All the values are given in \textperthousand relative to PDB. Repetitive analysis of the NBS 19 and internal laboratory standards revealed an external analytical error within $\pm 0.05\text{\textperthousand}$. Accelerator Mass Spectrometer (AMS) ages were measured on the same foraminifers picked up from five sediment intervals, using the NOSAMS facility at Woods Hole, USA. The radiocarbon ages were calibrated to the calendar ages, using calib 5.02 (Stuiver *et al.*, 2005); calendar ages are discussed throughout the study (Table 1). High resolution magnetic measurements were made on 175 sediment intervals using facilities at the Dr. K. S. Krishna Geomagnetic Research Laboratory, Allahabad, following the detailed methodology reported in Kumar *et al.* (2005). The three-point averages of all these parameters and their distributions are shown in Fig. 4.

For inorganic elemental chemistry, powdered sediments were weighed accurately to ~ 100 mg, transferred to clean Teflon beakers and open acid digestion was carried out at GSJ, Tsukuba. The sediments were repeatedly digested by treating with a mixture of HCl, HNO_3 , HClO_4 and HF under controlled conditions. Finally, 3 ml of HNO_3 was added to the digested samples and the entire solution was brought to a standard volume. Major and minor elements were measured using ICP-AES (Seiko SPS 7800) and trace elements using ICP-MS (Yokogawa Analytical Systems PMS-200) at GSJ, Tsukuba. Accuracy and reproducibility were confirmed by repeated measurement of the GSJ internal standards, JA2, JB2, JG1A and JR1. Reproducibility of the meas-

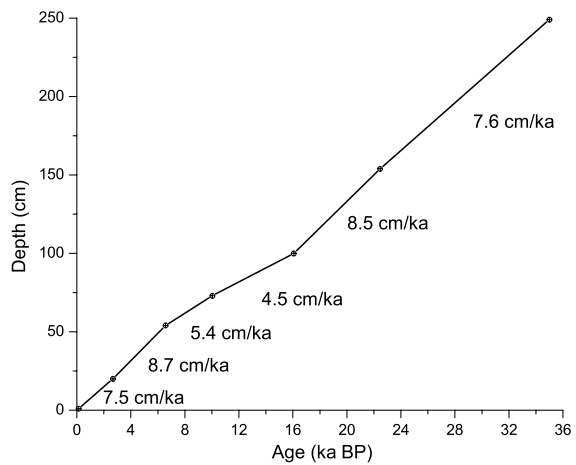


Fig. 2. Depth vs. age of the sediments in core SK 148/4. Sedimentation rates for different intervals are also shown. Ages of the sediment intervals dated are shown in Table 1.

urements for all elements reported here was better than $\pm 8\%$. Following the seminal works of other investigators on the geochemistry of the sediments of the Arabian Sea (Hermelin and Shimmield, 1990; Shimmield and Mowbray, 1991; Reichart *et al.*, 1997; Schnetger *et al.*, 2000; Van der Weijden *et al.*, 2006), elements were classified into terrigenous (Fe, K, Rb, Sc, Zn, Th and V), biogenous and organic-associated (CaCO_3 , OC, Sr, Cu, Ni, Zn, Sr, Ba) and redox-sensitive elements (Mo, U and Cd). In order to correct for dilution by terrigenous sediment component, element concentrations were normalized by Al and their down core distributions are shown in Figs. 5–7.

3. Results

3.1 Chronology and sedimentation rates

The age model of the core is based on five calibrated AMS ^{14}C dated intervals and comparison of our $\delta^{18}\text{O}$ record in marine isotope stage (MIS) 3 interval with that

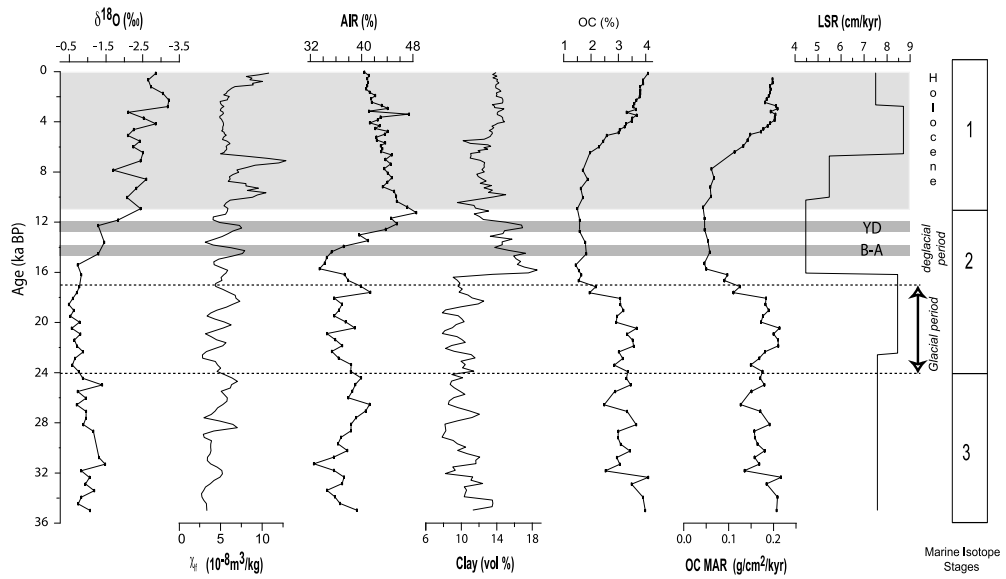


Fig. 3. Down-core variations of $\delta^{18}\text{O}$, χ_{lf} , acid-insoluble residue (AIR), clay volume, organic carbon (OC), mass accumulation rate (MAR) of OC and linear sedimentation rates (LSR) in core SK 148/4, YD - Younger Dryas, B-A - Bølling-Allerød event, Marine isotope stages 1, 2 and 3 are also shown.

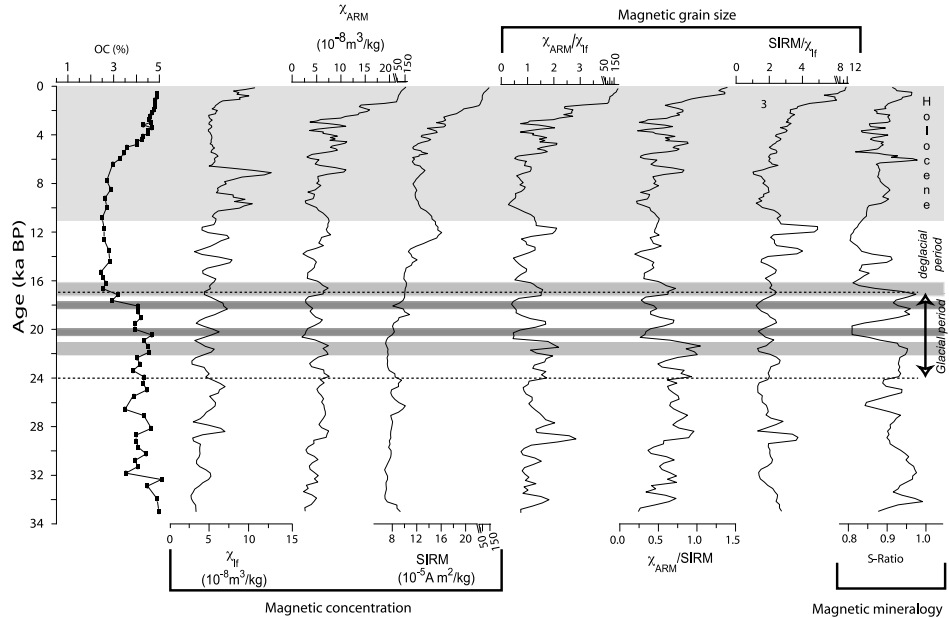


Fig. 4. Down-core variations of percent OC and rock magnetic concentration, grain size and mineralogy parameters in core SK 148/4.

of SPECMAP. The top 250 cm of the core sediments represent the last 35 kaBP, deposited at ~ 7 cm/ka. The rates of sedimentation for different intervals of the core vary from 4.5 cm/ka to 8.7 cm/ka, and are highest for the glacial and late Holocene sediments, and lowest for deglacial and early Holocene sediments (16–6.6 kaBP - Fig. 2).

3.2 Variations in $\delta^{18}\text{O}$, χ_{lf} , acid-insoluble residue, clay, OC and CaCO_3

The $\delta^{18}\text{O}$ stratigraphy of the core is admittedly a low resolution record because of low sedimentation rates. The $\delta^{18}\text{O}$ values in MIS 3 are lighter, $-0.75\text{\textperthousand}$ to $-1.5\text{\textperthousand}$, and gradually become heavier towards the Last Glacial

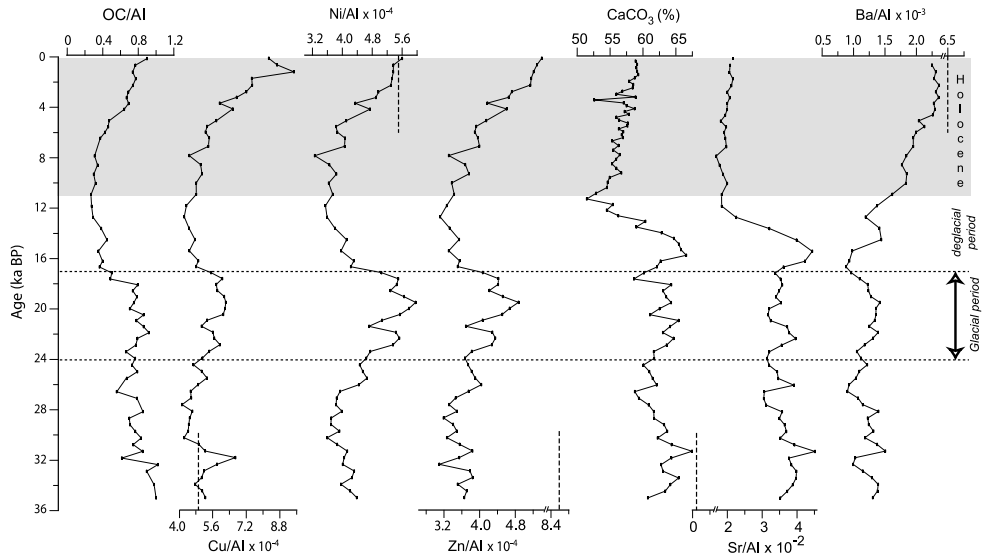


Fig. 5. Down-core variations of OC/Al, Cu/Al, Ni/Al, Zn/Al, CaCO₃, Sr/Al, and Ba/Al in core SK 148/4. Small vertical dashed line is the Al-normalized ratio of the Post-Archean Australian Shale (PAAS).

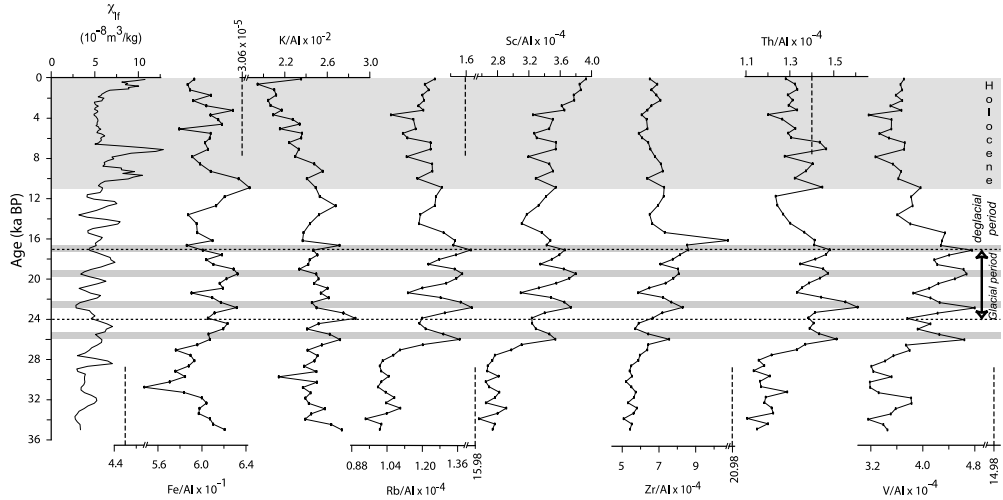


Fig. 6. Down-core variations of χ_{lf} , Fe/Al, K/Al, Rb/Al, Sc/Al, Zr/Al, Th/Al, and V/Al in core SK 148/4. Small vertical dashed line is the Al-normalized ratio of the Post-Archean Australian Shale (PAAS).

Maxima (LGM), with the heaviest value of $-0.5\text{\textperthousand}$ at 18.2 kaBP (Fig. 3). The $\delta^{18}\text{O}$ excursion to low values starts during deglaciation and occurs gradually in three steps, punctuated by heavier values at 15.5 and 12.1 kaBP. The $\delta^{18}\text{O}$ values further reduce to $-2.5\text{\textperthousand}$, $-2.7\text{\textperthousand}$ and $-3.2\text{\textperthousand}$ at ~ 11.5 kaBP, ~ 8.8 kaBP and ~ 3 kaBP, respectively. The $\delta^{18}\text{O}$ resembles that of the global $\delta^{18}\text{O}$ signal during a warm period, except that the values are more negative. The acid-insoluble residue (AIR) content is lowest during MIS 3, slightly higher during the LGM, with a minor peak of high values between 18 and 16 kaBP. AIR starts

increasing at ~ 15.7 kaBP with an increase in the reduction of $\delta^{18}\text{O}$ and attains the highest value at ~ 11 kaBP. Thereafter it shows a decreasing trend towards the core top. Silt is the dominant component in MIS 3 and LGM sediments. The total clay volume is low in the sediments between 36 and 16 kaBP, but increases sharply to high values between ~ 16 and 12 kaBP with a minor trough of low values between 12 and 10 kaBP (Fig. 3). The low-frequency magnetic susceptibility (χ_{lf}) varies between 15 and $3 \times 10^{-8} \text{ m}^3/\text{kg}$, with peaks of high χ_{lf} and troughs of low χ_{lf} throughout the core. Larger peaks of high χ_{lf} co-

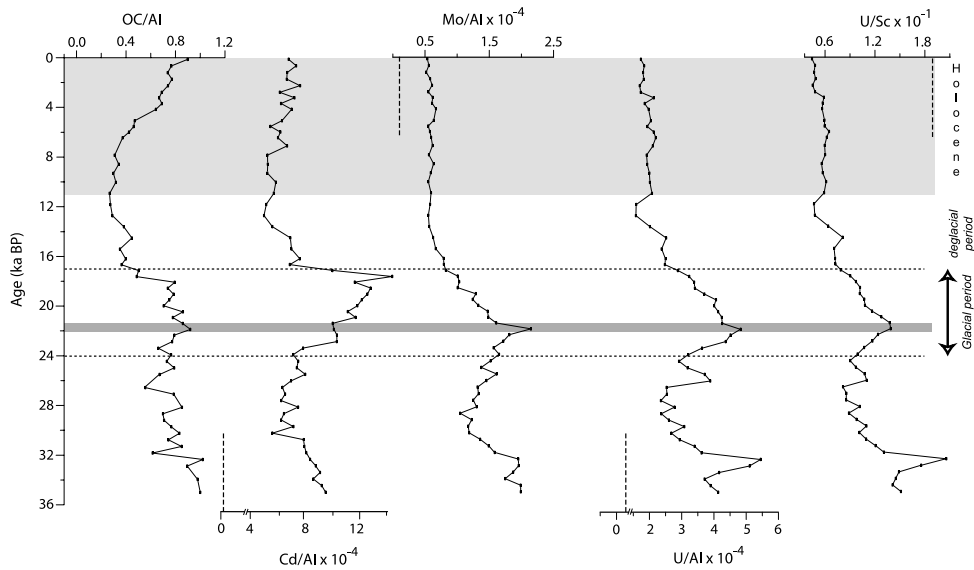


Fig. 7. Down-core variations of OC/Al, Cd/Al, Mo/Al, U/Al and U/Sc in core SK 148/4. Small vertical dashed line is the Al-normalized ratio of the Post-Archean Australian Shale (PAAS).

Table 2. Correlation coefficient of Al-normalized ratios of biogenic/organic elements.

Element/ Period	OC vs. Cu/Al	OC vs. Ni/Al	OC vs. Zn/Al	OC vs. Ba/Al	CaCO ₃ vs. Ba/Al	OC vs. CaCO ₃
Holocene	0.9	0.94	0.95	0.94	0.83	0.50
<11 kaBP	(n = 18)	(n = 27)				
Deglacial	0.76	0.71	0.81	0.35	-0.61	0.09
11–17 kaBP	(n = 8)	(n = 9)				
Glacial	-0.35	-0.24	-0.26	0.51	0.60	0.5
17–24 kaBP	(n = 14)	(n = 14)	(n = 14)	(n = 17)	(n = 17)	(n = 17)
Pre-glacial	-0.05	0.11	0.34	0.27	0.61	0.04
24–35 kaBP	(n = 15)	(n = 16)				

incide with strongly reduced $\delta^{18}\text{O}$ values during the Holocene. Several peaks of high χ_{lf} occur both in deglacial and glacial sediments. A broad trough of low OC values amid high OC values during the glacial and late Holocene sediments is characteristic of the core. OC starts decreasing from 18 kaBP, maintaining low values until 10.5 kaBP and then increases gradually towards the core top. The mass accumulation rates (MAR) of OC follow that of OC distribution. The ratio of organic carbon to total nitrogen is broadly in the range 7–11, which is indicative of marine OC throughout the core.

3.3 Rock magnetic properties

Magnetic mineral concentrations are high for the sediments at the core top and decrease towards the bottom. Low-frequency magnetic susceptibility (χ_{lf}) reflects bulk concentrations of magnetizable material and is also

related to the grain size of magnetic components. It exhibits several narrow and broad peaks of high χ_{lf} and broad troughs of low χ_{lf} throughout the core (Fig. 4). The anhysteretic susceptibility (χ_{ARM}) and Saturation isothermal remnant magnetization (SIRM) provide information on concentrations, but their ratio with χ_{lf} is largely related to grain size (Oldfield, 1991). The χ_{ARM} values are $\sim 150 \times 10^{-8} \text{ m}^3/\text{kg}$ at the core top but decrease sharply to $15 \times 10^{-8} \text{ m}^3/\text{kg}$ within the top 10 cm of the sediment (2 kaBP). It fluctuates broadly between 2.5 and $7.5 \times 10^{-8} \text{ m}^3/\text{kg}$ in the remaining portion of the core. SIRM is also high at the core top, but is distributed mostly around decreased values; its down-core decrease is quite distinct. The S-ratio is related to the proportions of low-coercivity to high-coercivity magnetic minerals. The sediments of the last 7 kaBP exhibit a broad trough of low values of magnetic concentration, grain size and mineralogy vari-

ables and correspond to high OC (4.1–1.2%). The sediments between 7 and 17 kaBP are characterized by a broad trough of low OC, accompanied by narrow peaks of high χ_{lf} and matching peaks in other magnetic concentration, grain size and mineralogy parameters. The peak in χ_{lf} profile at 10 kaBP is represented by a broad trough of low values in χ_{ARM} , SIRM, χ_{ARM}/χ_{lf} and $\chi_{ARM}/SIRM$ and reduced S-ratio. The sediments of 17–35 kaBP contain high OC. The peaks in χ_{lf} do not resemble those in χ_{ARM} and SIRM at several intervals both in 7–17 kaBP and 17–35 kaBP. Small, narrow, low amplitude peaks in χ_{lf} centered at ~17 and 22 kaBP correspond to large, broad peaks of high χ_{ARM} , and increased χ_{ARM}/χ_{lf} , $\chi_{ARM}/SIRM$ and high S-ratios (light bands in Fig. 4). The peaks in χ_{lf} profile at ~18 kaBP, ~20 kaBP (dark bands in Fig. 4) and to some extent ~25 kaBP match with low χ_{ARM} , SIRM, χ_{ARM}/χ_{lf} , $\chi_{ARM}/SIRM$ and decreased S-ratio. The peaks in χ_{lf} profile at ~28 kaBP are represented by minor peaks in χ_{ARM} and SIRM profiles and low S-ratios.

3.4 Variations in biogenic, terrigenous and redox-sensitive elements

For convenience of description the core is divided into sections, as shown in Figs. 3–7. The section boundaries do not correspond with marine isotope stages but overlap one another. The element/Al concentrations of Rb, Zr, V, Ba, and Zn are lower and Fe, K, Ca, Sr, Mo and U are higher than that of shale at different sediment intervals (see Figs. 5–7). The Al-normalized profiles of Cu, Ni and Zn appear to imitate that of OC, and Sr with CaCO_3 (Fig. 5). OC exhibits a strong correlation with Ba/Al, Cu/Al, Ni/Al and Zn/Al and a moderate correlation with CaCO_3 in Holocene sediments. Ba/Al shows a strong correlation with CaCO_3 (Table 2; Fig. 5). OC shows a good correlation with Cu/Al, Ni/Al and Zn/Al, a weak correlation with Ba/Al and no correlation with CaCO_3 for the deglacial (17–11 kaBP) sediments. CaCO_3 is negatively correlated with Ba/Al in these sediments. OC shows no correlation with Cu/Al, Ni/Al and Zn/Al for the glacial (17–24 kaBP) and pre-glacial (24–35 kaBP) sediments. It correlates moderately with Ba/Al and CaCO_3 for the glacial sediments but weakly with pre-glacial sediments (Table 2). The Al-normalized ratios of Fe, K, Rb, Sc, Zr, Th and V show distinct highs and lows: large peaks of high ratios of these elements match with low χ_{lf} in glacial sediments, and peaks of low ratios of these elements match with peaks of high χ_{lf} (Fig. 6). The Mo, U and Cd values at different intervals in the core range from 2.4 to 7.9 ppm, 7 to 21.8 ppm and 0.22 to 0.57 ppm, respectively. Sirocko *et al.* (2000) reported Mo, U and Cd concentrations up to 6.29 ppm, 12 ppm and 0.8 ppm, respectively, for modern and Holocene sediments of the SW margin of India. The peak U/Al, Cd/Al and Mo/Al ratios are higher by factors of 2.0, 2.5 and 4, respectively, in

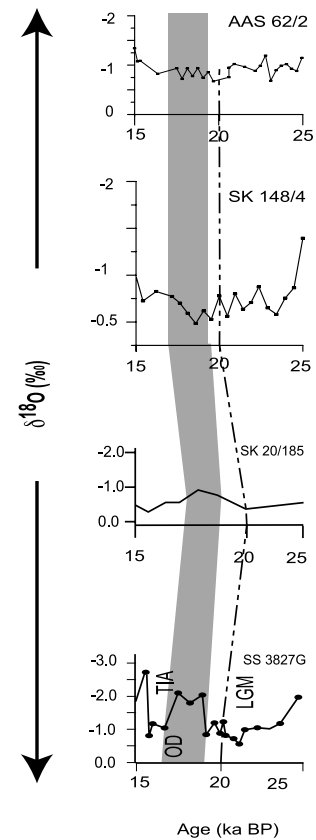


Fig. 8. $\delta^{18}\text{O}$ records of *Globigerinoides ruber* between 15 and 25 kaBP in different sediment cores in the southeastern and equatorial Arabian Sea. SK 148/4 - this paper, SK 20/185 (Sarkar *et al.*, 1990), AAS 62/2 (Rao *et al.*, 2008) and SS 3827G (Tiwari *et al.*, 2005). Note scale change both in X-axis and Y-axis for each graph.

glacial sediments than those in the Holocene. The Mo distribution replicates that of U. The U/Al and Mo/Al ratios peak at ~32 kaBP and then decrease until 25 kaBP. Thereafter their ratios increase progressively until 22 kaBP and then decrease gradually until 17 kaBP (Fig. 7). Their ratios are consistently low and decrease uniformly during the Holocene. The distribution of Cd is broadly similar to that of U and Mo, except that its maximum concentration occurs at 17 kaBP.

4. Discussion

4.1 Climatic and oceanographic conditions

The $\delta^{18}\text{O}$ values are heaviest in LGM sediments and lightest in Holocene, with a $\Delta\delta^{18}\text{O}$ amplitude of -2.2‰ (Fig. 3). Duplessy (1982) reported weaker SW monsoon (SWM) and a stronger NE monsoon (NEM) in the northern Indian Ocean during LGM than in the present day. The enhanced NE winds during the NEM cause high pre-

cipitation over the southeast Peninsular India and bring large quantities of fresh water to the SW Bay of Bengal. These low-saline waters are transported to the SE Arabian Sea by the northeast monsoon current (NEMC) and West India Coastal Currents (WICC) (see current direction in Fig. 1). Owing to the fact that weaker SWM and stronger NEM existed during LGM and the location of the core is in an area under the influence of NEMC and WICC, one would expect lighter $\delta^{18}\text{O}$ values for near-surface dwelling *Globigerinoides ruber* during the LGM. The heaviest $\delta^{18}\text{O}$ values, however, suggest that the NEM might not have been stronger during the LGM. Tiwari *et al.* (2005) reported a significant reduction in $\delta^{18}\text{O}$ ($\sim 1.5\text{\textperthousand}$) during 19–17 kaBP in a core SS 3827G from the equatorial Arabian Sea (Figs. 1 and 8) and attributed this reduction to the strong influence of low-saline waters brought by the NEMC. The maximum reduction in $\delta^{18}\text{O}$ for *G. ruber* during 21–17 kaBP is found to be $\sim 0.25\text{\textperthousand}$ in core SK 148/4, $\sim 0.25\text{\textperthousand}$ in core AAS 62/2 and $\sim 0.5\text{\textperthousand}$ in core SK 20/185 (see Fig. 8). This suggests that the effect of low-saline, Bay of Bengal waters is least along the SW margin of India during LGM and perhaps more towards the west, away from the margin. Alternatively, convective mixing due to stronger NEM during LGM may have quickly mixed up the surficial cap of low-saline waters and nullified its effect on $\delta^{18}\text{O}$. Stronger convective mixing causes injection of nutrients into the euphotic zone and increases productivity. Relatively high organic carbon and Ba/Al ratios in glacial sediments do indeed attest to high productivity (see below). The $\delta^{18}\text{O}$ excursion towards lighter values at ~ 15.7 kaBP coincides with an increase in acid-insoluble residue (AIR) content and clay volume (Fig. 3); this may represent river input and enhancement of the summer SW monsoon, as also reported by several investigators in this region (Thamban *et al.*, 2001; Sinha *et al.*, 2005; Tiwari *et al.*, 2005; Rao *et al.*, 2008).

By comparing the records of $\delta^{18}\text{O}$, magnetic susceptibility (χ_{lf}) and OC it is possible to infer some global climatic events. The Bølling-Allerød (B-A) event at 15.5–13 kaBP, a warming event, is reflected in our core by reduced $\delta^{18}\text{O}$ values, a strong peak in χ_{lf} and relative increases in OC, Ba/Al, Sr/Al and CaCO_3 (Figs. 3 and 5), indicating an increase in monsoon precipitation and productivity during this time. Sinha *et al.* (2005) suggested that the SW Indian monsoon precipitation during the B-A event was coupled with the variations in the East Asian monsoon and North Atlantic climate. Similarly, the gradual reduction in $\delta^{18}\text{O}$ at ~ 13.7 –11.8 ka was interrupted by heavier $\delta^{18}\text{O}$ at ~ 12 kaBP (Fig. 3), which correspond to the mid-point of a peak in χ_{lf} profile (Fig. 3). This interval is assigned as a Younger Dryas (YD) event that has been reported in sediments of the eastern Arabian Sea (von Rad *et al.*, 1999; Singh *et al.*, 2006; Rao *et al.*, 2008).

The presence of Younger Dryas and B-A events similar to that of North Atlantic and Northwestern Arabian Sea (Schulte *et al.*, 1999; von Rad *et al.*, 1999) reflect abrupt climatic changes that are of global origin, suggesting common forcing agents through atmospheric circulation. At the end YD event, $\delta^{18}\text{O}$ values were further reduced during the early Holocene and peaked at ~ 11.5 ka, 9 ka and 7 kaBP with intermittent low values, suggesting that a major intensification of summer SWM occurred at 11.5 kaBP, synchronous with a major climate transition recorded in Greenland (Sirocko *et al.*, 1993). The greater reduction of $\delta^{18}\text{O}$ and strong χ_{lf} peaks between 11.5 and 7 kaBP suggest that the intensified monsoon persisted during this period.

4.2 Productivity and redox conditions

4.2.1 Glacial sediments

The OC values are high and similar in glacial and late Holocene sediments (Fig. 5), despite the fact that the southwest monsoon (SWM) was stronger during the Holocene and weaker during the last glaciation (Van Campo *et al.*, 1982). The role of low-oxygenated bottom waters (Sarkar *et al.*, 1993; Van der Weijden *et al.*, 1999; Agnihotri *et al.*, 2003; Pattan *et al.*, 2003) and/or high productivity linked to the NE monsoon winds during LGM (Rostek *et al.*, 1997; Schulte *et al.*, 1999; von Rad *et al.*, 1999; Thamban *et al.*, 2001) were suggested to be responsible for organic-rich sediments in the Eastern Arabian Sea. Since the organic matter content in sediments is also influenced by other factors (quality of organic matter, early diagenesis, rates of sedimentation and sediment type—see Paropkari *et al.*, 1992), it may not serve as an independent proxy for productivity. Schnetger *et al.* (2000) showed that total organic carbon is not a tracer, but Ba/Al serves as a proxy for paleoproductivity in the sediments of the deep Arabian Sea. Sediment trap experiments showed that Ca, Sr and Ba associate with biogenic particles, and particulate organic matter is an effective scavenger for metals such as Cu, Ni, Zn and V, the concentrations of which are controlled by seasonally driven changes in primary productivity (Jickells *et al.*, 1984; Shimmield and Mowbray, 1991; Schnetger *et al.*, 2000). Ba in the offshore precipitates as barite from the living phytoplankton cells and thus barite content in sediments is a function of biological productivity. Dymond *et al.* (1992) suggested that excess Ba in sediments may serve as a proxy for particulate organic carbon (POC). Prakashbabu *et al.* (2002) reported excess Ba in Holocene sediments of the SW margin of India and suggested that, although Ba is lost during sub-oxic diagenesis, it reflects productivity trend on this margin. Tracers such as Ba/Al (Shimmield *et al.*, 1990; Hermelin and Shimmield, 1990), Zn/Al and Ba/Al (Reichart *et al.*, 1997), Ni/Al and Zn/Al (von Rad *et al.*, 1999) and Cu/Al (Schnetger *et al.*, 2000)

along with OC have been used as paleoproductivity indicators in the Arabian Sea. Although OC/Al and Ba/Al profiles show an opposite trend in deglacial sediments of core SK 148/4 (Fig. 5), OC showed a moderate correlation with Ba/Al ($r = 0.51$) and CaCO_3 ($r = 0.5$), but no correlation with Cu/Al, Ni/Al and Zn/Al ratios ($r = -0.24$ to -0.35) for the glacial sediments. All these elements, however, showed a strong correlation with OC for Holocene sediments (Table 2). As Ba/Al also correlates well with CaCO_3 ($r = 0.6$), biological productivity seems to be an important factor for organic enrichment in glacial sediments. The poor correlation of Cu, Ni and Zn with OC may be due to their diagenetic mobilization and redistribution during reducing conditions (see below). Barite is lost in sub-oxic conditions and is dissolved under anoxic sediments. The higher mass accumulation rate of OC (Fig. 3) and Ba may have preserved some OC and Ba, leading to a moderate correlation. Schenau *et al.* (2001) suggested that the burial efficiency of barite depends on the degree of barite saturation and barite accumulation rate. Chase and Anderson (2001) investigated U concentrations in 50 sediment cores over a wide latitude and depth range in the Atlantic sector of the Southern Ocean and suggested that authigenic U in glacial sediments cannot be due entirely to the lateral supply of POC via sediment focusing or reduction in bottom water oxygen concentrations, but reflects primarily increased particulate organic carbon. Comparison of U/Al, Th/Al and U/Sc profiles (Figs. 6 and 7) indicates enrichment of authigenic U in glacial sediments (see below) and thus high organic flux, supporting productivity. Higher surface productivity in glacial times than in deglacial times was suggested to be due to deep convective mixing related to intensified winter monsoon winds (see Rostek *et al.*, 1997; Reichart *et al.*, 2002).

The concentrations of Mo, U and Cd are 2 to 4 times greater in glacial sediments than those in the Holocene (Fig. 7). These redox-sensitive metals are initially supplied from terrestrial sources via runoff from land or dust input, and are scavenged to the seafloor by adsorption onto sinking particulate flux, such as plankton organic materials (OM), Fe-, and Mn-oxides and clays (Morford and Emerson, 1999; Nameroff *et al.*, 2002). Their enrichment in sediments depends on concentration gradients of metals, depth of the redox boundaries below the sediment-water interface, mass accumulation rates and bioturbation depths. The metals liberated during microbial decomposition of OM during early diagenesis may escape into pore water and then to overlying waters, or diffuse downwards and precipitate in the anoxic zone, depending on the redox characteristics of the respective elements. Therefore, their enrichment occurs immediately below the oxic/sub-oxic boundary, or at deeper depths in sediments (Thomson *et al.*, 2001). U usually occurs as U(VI), reduces to U(IV)

close to the reduction of Fe(III) to Fe(II) and then precipitates in the sediments (Morford and Emerson, 1999). The highest U/Al coinciding with low Fe/Al at 22 kaBP (see Figs. 6 and 7) suggests that U reduction may have occurred with reduced Fe(III). Zheng *et al.* (2000) suggested that, although the authigenic precipitation of U is independent of sulphide production, HS created during sulfate reduction could also be a reducing agent for U(VI). Sc is largely associated with terrigenous material, The U/Sc distribution follows that of U/Al (Fig. 7), suggesting that a high U content is due to authigenic enrichment in reducing conditions. It has been suggested that the Mo liberated to the pore waters does not enrich in sub-oxic sediments but precipitates as an authigenic phase in anoxic sediments only when sulphate reduction becomes important (Crusius *et al.*, 1996; Chaillou *et al.*, 2002). The gradual increase of both U/Al and Mo/Al from 24 to 22 kaBP (Fig. 7) suggests an increase in reductive diagenesis with strong anoxic conditions at ~ 22 kaBP. The presence of fine-grained ferrimagnetic mineral at this interval is also an indication of a strong anoxic environment (see Subsection 4.3). Cd is usually associated with plankton organic matter (OM), released to the pore waters during OM degradation and removed from solution as CdS even with trace sulphide under anoxic conditions. Cd enrichment is thus a good indicator of sulphide production (Rosenthal *et al.*, 1995). The maximum Cd peak (at 17 kaBP) is located close to the glacial/deglacial boundary and spatially separated from maximum U/Al and Mo/Al peaks that occur at ~ 22 kaBP. The gradual Cd enrichment indicates sulfate reducing conditions. The pronounced shift in Cd peak (Fig. 7) may be due to fluctuating input of organic matter that results in a shift of the position of the redox boundary (see Gobeil *et al.*, 1997), and precipitation of Cd as CdS in the presence of trace amounts of H_2S . Schnetger *et al.* (2000) reported a Cd peak closer to the interface between the turbidite and pelagic carbonate sediment in the Arabian Sea and attributed it to the sensitive response of Cd to the changing redox conditions. Rock magnetic parameters indicate changing redox conditions in glacial sediments (see Subsection 4.3). Coarse fraction studies indicate a lack of bioturbation and the presence of dwarf benthic foraminifers, *Bulimina* sp., *Uvigerina* and *Bolivina*, suggesting oxygen-depleted bottom water conditions favouring reducing sedimentary conditions during the glacial period.

Glacial sediments exhibiting alternate peak high and low ratios of Fe/Al, K/Al, Rb/Al, Sc/Al, Zr/Al, Th/Al and V/Al, where the high ratios do not coincide with peak high χ_{lf} but with low χ_{lf} (see bands in Fig. 6), suggest different source materials for magnetized material and detrital elements. Radioactive and heavy mineral placer sands (zircon, monazite, ilmenite and rutile) are abun-

dant in the coastal and shelf region (Mallik *et al.*, 1987). Iron-rich authigenic verdine and glaucony and phosphate facies have been reported on the shelf and upper slope of the study region (Rao *et al.*, 1993). Heavy minerals and green clays concentrate in coarser sediments, whereas magnetized material concentrate in finer sediments. Peak high ratios of element/Al of Fe, K, Rb, Sc, Zr, Th and V could have been caused by the reworking of green clays and placer minerals from the emergent shelf and upper slope during low stands of sea level and thus exhibit enrichment at different sediment intervals than that of χ_{lf} . A narrow shelf (60 km) and steep continental slope (Rao and Wagle, 1997) favour this process and have been reported by Von Stackelberg (1972) and Thamban *et al.* (1997) in this region. These observations imply intermittent pulses during which the upper slope sediments are reworked, which controlled the peak high detrital element/Al ratios of K, Rb, Sc, Zr, Th and V (Fig. 6). Reworking of upper slope sediments thus also have contributed to the enrichment of OC in glacial sediments than in deglacial times. Sedimentation rates are also high in glacial sediments (Fig. 2). In other words, high biological productivity induced low-oxygenated bottom waters and reducing sedimentary conditions, reworking of upper slope sediments, high sedimentation rates and lack of bioturbation are responsible for organic-rich glacial sediments.

4.2.2 Deglacial sediments (17–11 kaBP)

This period in general is characterized by a rise in global sea level, abrupt climatic events, and rapid fluctuations in climate at the Pleistocene–Holocene boundary. Despite the lowest sedimentation rates (4.5 cm/ka), which prevent resolution of climatic events, the B-A event and Younger Dryas event can be discerned (Fig. 3). The planktonic $\delta^{18}\text{O}$ excursion to low values correlates well with the increase in Ba/Al ratio, a feature also observed by several others in sediment cores from different parts of the Arabian Sea (see Shimmield and Mowbray, 1991; Reichart *et al.*, 1997; Schnetger *et al.*, 2000; Pattan *et al.*, 2003). As Ba, excess Ba or Ba/Al ratio have been used as a proxy for productivity in the Arabian Sea, the elevated Ba/Al ratio has been attributed to high productivity due to increased upwelling and/or increased runoff and nutrient supply during interglacial periods (see Weedon and Shimmield, 1991; Shimmield, 1992; Reichart *et al.*, 1997; Schnetger *et al.*, 2000). The Ba/Al ratio is negatively correlated with OC (Table 2), however. The concentrations of redox-sensitive elements are also low in this part of the core (profiles of Cu, Ni, Zn, U, Mo, Cd in Figs. 5 and 7). The lowest sedimentation rates make the sediments in this part of the core more susceptible to “burn-down” of organic matter, so post-depositional oxygenation of organic carbon and redistribution of elements is perhaps responsible for low OC, Cu, Ni, Zn, Cd, Mo and U. The

increased AIR content and total clay volume (Fig. 3) attest to the increase in terrigenous influx that may have diluted OC in bottom sediments.

4.2.3 Holocene sediments

Strong peaks of high χ_{lf} (Fig. 4), low concentrations of OC, Cu, Ni, Zn, Ba, CaCO_3 (Fig. 5), and pulses of relatively high peaks of Th/Al, Sc/Al, Rb/Al and to some extent K/Al (Fig. 6) during the early Holocene suggest increased terrigenous flux and decreased biogenic or organic-associated flux. Strongly reduced $\delta^{18}\text{O}$ values (Fig. 3) suggest a maximum intensity of the southwest monsoon during this period. The wet, warm climate might have resulted in strong chemical weathering and influx of detrital matter from the land. The progressive increase in OC, Ba/Al, Cu/Al, Ni/Al and Zn/Al from early to late Holocene, and strong correlation of OC with all these elements (Table 2) and CaCO_3 ($r = 0.83$) suggest increasing surface productivity. Stronger SW monsoon winds may have induced strong coastal upwelling (Van Campo *et al.*, 1982), which resulted in high productivity in surface waters and burial of high OC and other productivity related or organic-associated elements. Despite the prevalence of oxygenated bottom waters in the Holocene and the present day, OC values are high in the late Holocene, similar to the glacial sediments that experienced reducing conditions (Fig. 5). This suggests that productivity is a major controlling factor for organic-rich sediments. Lower concentrations of U, Mo and Cd in the Holocene than in glacial sediments (Fig. 7) suggest that the Holocene sediments could not achieve strong reducing conditions thanks to the oxygenated bottom waters.

4.3 Role of diagenesis in dissolution and precipitation of magnetic minerals

Liu *et al.* (2004) identified four stages of sediments that correspond to the affects of progressive early diagenesis. Stage 1 is least affected by diagenesis with high concentrations of detrital magnetite and hematite. Stage 2 shows the presence of pyrite and decreasing concentrations of detrital magnetite. Stage 3 is marked by a progressive loss of hematite with depth and minimum magnetite and stage 4 with enhanced concentrations of authigenic magnetic minerals such as greigite or pyrrhotite. The profiles of magnetic parameters (Fig. 4) exhibit all stages of diagenesis, but not in sequence as one proceeds down the core. (a) A trough of low values of all magnetic concentration, grain size and mineralogy variables in sediments of the last 7 kaBP indicates stage 2 diagenesis. High OC and relatively high rates of sedimentation (Figs. 2 and 3) may have favoured reductive diagenesis and dissolution of magnetic minerals, a process that has been documented in numerous studies (Leslie *et al.*, 1990; Karlin, 1990; Bloemendal *et al.*, 1993; Kumar *et al.*, 2005; Rao *et al.*, 2008). (b) High amplitude peaks

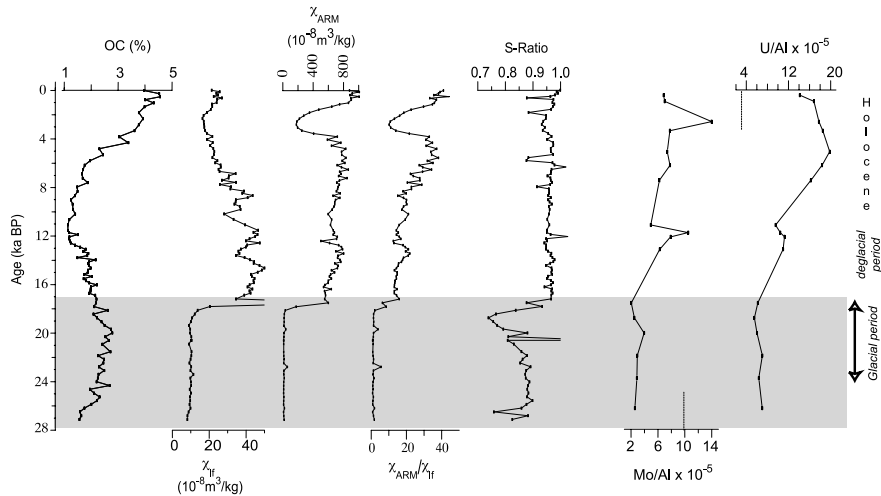


Fig. 9. Down-core variations of OC, rock magnetic concentration (χ_{lf} , χ_{ARM}), grain size (χ_{ARM}/χ_{lf}) and mineralogy (S-ratio) parameters, and Mo/Al and U/Al ratios in core AAS 62/2 (modified after Rao *et al.*, 2008).

in χ_{lf} with parallel peaks in χ_{ARM} , SIRM, and S-ratio between 7 and 11 kaBP are associated with low OC and peaks of high concentrations of terrigenous elements (Figs. 4 and 6). This part may represent the least diagenesis of magnetic minerals and corresponds to stage 1 of Liu *et al.* (2004). (c) The peaks of high χ_{lf} at ~10 ka, 18 ka, 20 ka and 25 ka match with low χ_{ARM} , SIRM, χ_{ARM}/χ_{lf} , χ_{ARM} /SIRM and S-ratio (see Fig. 4). The decrease in χ_{ARM} and grain size ratios could mean that the fine-grained magnetite particles are selectively dissolved during early diagenesis. This corresponds to stage 2/3 diagenesis (Liu *et al.*, 2004). (d) For a given χ_{lf} peak, χ_{ARM} , χ_{ARM}/χ_{lf} , χ_{ARM} /SIRM peaks have increased at certain intervals (~17 and ~22 kaBP), indicating an increase of fine-grained ferrimagnetites (see Fig. 4). High S-ratios (of ~0.95) indicate the dominance of an extremely low-coercivity magnetic phase. Variations in grain size can be caused by compositional sorting during sedimentation or variation in the proportion of authigenic magnetic minerals such as greigite or pyrrhotite in a typical anoxic environment, or caused by magnetotactic bacterial enhancement below redox fronts (Roberts *et al.*, 1996; Hounslow and Maher, 1999; Rey *et al.*, 2005). These intervals are associated with highest concentrations of U/Al, Mo/Al and Cd/Al (see Fig. 7) indicating strong sulphate reducing conditions (see above). High S-ratios may not be related to detrital fine-magnetite or biogenic bacterial magnetite, as these magnetic phases become dissolved under strong reducing conditions. The increased fine-grained ferrimagnetic phase may therefore be due to the formation of new magnetic mineral under strong redox conditions. Roberts (1995) pointed out that the occurrence of authigenic greigite in single domain-like state is typical of an anoxic environment, especially in the pres-

ence of numerous redox-sensitive elements. Greigites usually display high-coercivities, but the substitution of Ni and Cr in the crystal structure may give rise to low coercivities, relative to those documented for greigite (Roberts *et al.*, 1999). We therefore suggest that a new ferrimagnetic mineral, probably greigite, is forming at these intervals. The glacial sediments showing high OC, strong reducing anoxic conditions and new magnetic minerals appear analogous to the sapropels from the eastern Mediterranean Sea (Roberts *et al.*, 1999; Passier *et al.*, 2001) and thin light sediment layers in the Japan Sea (Vigliotti, 1997; Hayashida *et al.*, 2007), which are known for their diagenetic magnetic enhancement. The sediments of 17–24 kaBP thus showed intervals of magnetic dissolution (e.g. ~18, 20 and 25 kaBP—dark bands in Fig. 4) alternate with authigenic growth of secondary magnetic phases (~17 and 22 kaBP—light bands in Fig. 4); this may be due to the result of fluctuating redox conditions, reflecting paleoproductivity changes during this period.

The rock magnetic and geochemical record of this core SK 148/4 (Figs. 4 and 7) was compared with that of core AAS 62/2 (Fig. 9). Both cores exhibit stage 1 and 2/3 diagenesis at intervals in the Holocene. However, the records differ strongly during glacial times: Core AAS 62/2 exhibits high OC, distinctly low magnetic concentration, grain size and mineralogy parameters and low concentrations of Mo and U. Despite the development of reductive diagenetic conditions wherein magnetic minerals were dissolved, there is little enrichment of U and Mo (Fig. 9). This is due to remobilization of redox-sensitive elements into the water column thanks to intermittent bioturbation (Rao *et al.*, 2008). The 17–28 kaBP sediments of the core thus represent sulfate reduction to intermittent oxic conditions. On the other hand, the core

SK 148/4 shows intervals of reductive diagenesis alternating with intervals of enhanced authigenic ferrimagnetites (Fig. 4; Subsection 4.3) and high OC, Mo, U and Cd (Fig. 7; Subsection 4.2.1). Stronger reductive diagenesis, anoxic sedimentary conditions and low oxygenated bottom waters are characteristic of glacial sediments. While both the cores were recovered from nearly similar depths and oxygenated present-day bottom waters, sedimentary conditions during glacial periods, differed within 440 km (distance between two cores). This is due to differences in biological productivity, reworking of upper slope sediments and sedimentation rates. Using a suite of biomarkers (alkenones, dinosterol, brassicasterol) Schulte *et al.* (1999) revealed the presence of oxygenated bottom waters during the last 330 kyr in a core from the equatorial Indian Ocean, with varying intensity of the oxygen minimum zone (OMZ) (including the complete disappearance of OMZ at times) in a core from the northeastern Arabian Sea during the last 65 kyr. Using OC, Σ alkenone, $\delta^{13}\text{C}$ and $\delta^{15}\text{N}$ data in a core from the eastern Arabian Sea (off Goa) Banakar *et al.* (2005) showed increased productivity and reduced denitrification during the last glacial maximum (LGM). We therefore suggest that the prevalence of low oxygenated bottom water during glacial times should not be generalized.

Acknowledgements

We thank the Directors of the National Institute of Oceanography, National Centre for Antarctic and Ocean Research, Goa and Indian Institute of Geomagnetism, Mumbai for facilities and encouragement. Part of the geochemical work was carried out by Meloth Thamban (MT) at the Geological Survey of Japan, Tsukuba through financial support from the Japan Science Promotion Society (JSPS). MT thanks Prof. Hodaka Kawahata for extending the facilities. We thank Dr. C. Prakashbabu for organic carbon analyses. Part of this work was carried out from the project funds of Department of Science and Technology, New Delhi. We thank the reviewers of this paper for their insight and critical comments which improved our understanding of the processes suggested in the paper. This is NIO contribution 4624.

References

Agnihotri, R., M. M. Sarin, B. L. K. Somayajulu, A. J. T. Jull and G. S. Burr (2003): Late Quaternary biogenic productivity and organic carbon deposition in the eastern Arabian Sea. *Palaeogeo. Palaeoclimat. Palaeoecol.*, **197**, 43–60.

Banakar, V. K., T. Oba, A. R. Chodankar, T. Kusamato, M. Yamamoto and M. Minagawa (2005): Monsoon related changes in sea surface productivity and water column denitrification in the eastern Arabian Sea during the last glacial cycle. *Mar. Geol.*, **219**, 99–108.

Bloemendal, J., B. Lamb and K. W. King (1988): Paleoenvironmental implications of rock-magnetic proper- ties of late Quaternary sediment cores from the eastern equatorial Atlantic. *Paleoceanography*, **3**, 61–87.

Bloemendal, J., J. W. King, A. Hunt *et al.* (1993): Origin of sedimentary magnetic record at Ocean Drilling Program sites on the Owen Ridge, Western Arabian Sea. *J. Geophys. Res.*, **98**, 4199–4219.

Chaillou, G., P. Anschutz, G. Lavaux, J. Schafer and G. Blanc (2002): The distribution of Mo, U, and Cd in relation to major redox species in muddy sediments of the Bay of Biscay. *Mar. Chem.*, **80**, 41–59.

Chase, X. and R. F. Anderson (2001): Evidence from authigenic uranium for increased productivity of the glacial Subantarctic Ocean. *Palaeoceanography*, **16**, 468–478.

Clemens, S. C. and W. L. Prell (1990): Late Pleistocene variability of Arabian Sea summer monsoon winds and continental aridity: eolian records from the lithogenic component of deep sea sediments. *Paleoceanography*, **5**, 109–145.

Crusius, J., S. E. Calvert, T. Pederson and D. Sage (1996): Rhenium and Molybdenum enrichments in sediments as indicators of oxic, sub-oxic and sulfidic conditions of deposition. *Earth Planet. Sci. Lett.*, **145**, 65–78.

Duplessy, J. G. (1982): Glacial to interglacial contrast in the northern Indian Ocean. *Nature*, **295**, 494–498.

Dymond, J., E. Suess and M. Lyle (1992): Barium in deep sea sediments: a geochemical proxy for paleoproductivity. *Paleoceanography*, **7**, 163–181.

Gobeil, C., R. W. MacDonald and B. Sundby (1997): Diagenetic separation of cadmium and manganese in suboxic continental margin sediments. *Geochim. Cosmochim. Acta*, **61**, 4647–4654.

Hayashida, A., S. Hattori and H. Oda (2007): Diagenetic modifications of magnetic properties observed in a piston core (MD01-2407) from the Oki Ridge, Japan Sea. *Palaeogeo. Palaeoclimat. Palaeoecol.*, **247**, 65–73.

Hermelin, J. O. R. and G. B. Shimmield (1990): The importance of the oxygen minimum zone and sediment chemistry in the distribution of recent benthic foraminifera in the northwest Indian Ocean. *Mar. Geol.*, **91**, 1–29.

Hounslow, M. W. and B. A. Maher (1999): Source of the climate signal recorded by magnetic susceptibility variations in the Indian Ocean sediments. *J. Geophys. Res.*, **104**, 5047–5061.

Jickells, T. D., W. G. Deuser and A. H. Knap (1984): The sedimentation rates of trace elements in the Sargasso Sea measured by sediment traps. *Deep-Sea Res., Part A*, **31**, 1169–1178.

Karlin, R. (1990): Magnetite diagenesis in marine sediments from Oregon continental margin. *J. Geophys. Res.*, **95**, 4405–4419.

Kumar, A. A., V. P. Rao, S. K. Patil, P. M. Kessarkar and M. Thamban (2005): Rock magnetic records of the sediments of the eastern Arabian Sea: evidence for late Quaternary climatic change. *Mar. Geol.*, **220**, 59–82.

Leslie, B. W., S. P. Lund and D. E. Hammond (1990): Rock magnetic evidence for the dissolution and authigenic growth of magnetic minerals within anoxic marine sediments of the California continental borderland. *J. Geophys. Res.*, **95**, 4437–4452.

Liu, J., R. Zhu, A. P. Roberts, S. Li and J. H. Chang (2004):

High resolution analysis of early diagenetic effects on magnetic minerals in Post-middle Holocene continental shelf sediments from the Korea Straight. *J. Geophys. Res.*, **109**, B03103, 1–15.

Mallik, T. K., V. Vasudevan, P. A. Verghese and T. Machado (1987): The black sand placer deposits of Kerala beach, Southwest India. *Mar. Geol.*, **77**, 129–150.

Morford, J. L. and S. Emerson (1999): The geochemistry of redox sensitive trace metals in sediments. *Geochim. Cosmochim. Acta*, **63**, 1735–1750.

Nameroff, T. J., L. S. Balistrieri and J. W. Murray (2002): Suboxic trace elemental geochemistry in the eastern tropical North Pacific. *Geochim. Cosmochim. Acta*, **66**, 1139–1158.

Oldfield, F. (1991): Environmental magnetism—A personal prospective. *Quat. Sci. Rev.*, **10**, 73–85.

Paropkari, A. L., C. P. Babu and A. Mascarenhas (1992): A critical evaluation of depositional parameters controlling the variability of organic carbon in the Arabian Sea sediments. *Mar. Geol.*, **107**, 213–226.

Passier, H. F., G. J. de Lange and M. J. Dekkers (2001): Magnetic properties and geochemistry of the active oxidation front and the youngest sapropel in the eastern Mediterranean Sea. *Geophys. J. Inter.*, **145**, 604–614.

Pattan, J. N., T. Masuzawa, P. D. Naidu, G. Parthiban and M. Yamamoto (2003): Productivity fluctuations in the south-eastern Arabian Sea during the last 140 ka. *Palaeogeogr. Palaeoclimat. Palaeoecol.*, **193**, 575–590.

Prakashbabu, C., H.-J. Brumsack, B. Schnetger and M. E. Bottcher (2002): Ba as a productivity proxy in continental margin sediments: a study from the eastern Arabian Sea. *Mar. Geol.*, **184**, 189–206.

Prell, W. L., D. W. Murray and S. C. Clemens (1992): Evolution and variability of the Indian Ocean summer monsoon: Evidence from the Western Arabian Sea Drilling Program. In *Synthesis of Results from the Scientific Drilling in the Indian Ocean*, ed. by R. A. Duncan, D. K. Rea, R. B. Kidd, U. von Rad and J. K. Weissel, American Geophysical Union, *Geophysical Monograph*, **70**, 447–469.

Rao, V. P. and B. G. Wagle (1997): Geomorphology and surficial geology of the western continental shelf and slope of India: A review. *Curr. Sci.*, **73**, 330–350.

Rao, V. P., M. Lamboy and P. A. Dupeuble (1993): Verdine and other associated authigenic (glaucony, phosphate) facies from the surficial sediments of the southwestern continental margin of India. *Mar. Geol.*, **111**, 133–158.

Rao, V. P., P. M. Kessarkar, S. K. Patil and S. M. Ahmad (2008): Rock magnetic and geochemical record in a core from the eastern Arabian Sea: diagenetic and environmental implications during the late Quaternary. *Palaeogeogr. Palaeoclimat. Palaeoecol.*, **270**, 46–52.

Reichart, G. J., M. den Dulk, H. J. Visser, C. H. Vander Weijden and W. K. Zachariasse (1997): A 225 kyr record of dust supply, paleoproductivity and the oxygen minimum zone from the Murray Ridge (northern Arabian Sea). *Palaeogeogr. Palaeoclimat. Palaeoecol.*, **134**, 149–169.

Reichart, G. J., S. J. Schenau, G. J. de Lange and W. J. Zachariasse (2002): Synchronicity of oxygen minimum zone intensity on the Oman and Pakistan margins at sub-Milankovitch time scales. *Mar. Geol.*, **185**, 403–415.

Rey, D., K. J. Mohamed, A. Bernabeu, B. Rubio and F. Vilas (2005): Early diagenesis of magnetic minerals in marine terrestrial environments: geochemical signatures of hydrodynamic forcing. *Mar. Geol.*, **215**, 215–236.

Roberts, A. P. (1995): Magnetic properties of greigite (Fe_3S_4). *Earth Planet. Sci. Lett.*, **134**, 227–236.

Roberts, A. P., R. L. Reynolds, K. L. Veresub and D. P. Adam (1996): Environmental magnetic implications of greigite (Fe_3S_4) formation in a 3 m.y. lake sediment record from Butte Valley, northern California. *Geophys. Res. Lett.*, **23**, 2859–2862.

Roberts, A. P., J. S. Stoner and C. Richter (1999): Diagenetic magnetic enhancement of sapropels from the eastern Mediterranean Sea. *Mar. Geol.*, **153**, 103–116.

Robinson, S. G., J. T. S. Sahota and F. Oldfield (2002): Early diagenesis in North Atlantic abyssal plain sediments characterized by rock magnetic and geophysical indices. *Mar. Geol.*, **163**, 77–107.

Rosenthal, Y., P. Lam, E. A. Boyle and A. Thomson (1995): Authigenic Cd enrichments in suboxic sediments. Precipitation and post-depositional mobility. *Earth Planet. Sci. Lett.*, **132**, 99–111.

Rostek, F., E. Bard, L. Beaufort, C. Sonzogni and G. Ganssen (1997): Sea surface temperature and productivity record for the past 240 kyrs in the Arabian Sea. *Deep-Sea Res., Part II*, **44**, 1461–1480.

Sarkar, A., R. Ramesh, S. K. Bhattacharya and G. Rajogopalan (1990): Oxygen isotopic evidence for a stronger winter monsoon current during the last Glaciation. *Nature*, **343**, 549–551.

Sarkar, A., S. K. Bhattacharya and M. M. Sarin (1993): Geochemical evidence for anoxic deep water in the Arabian Sea during the last glaciation. *Geochim. Cosmochim. Acta*, **57**, 1009–1016.

Schenau, S. J., M. A. Prins, G. J. de Lange and C. Monnin (2001): Barium accumulation in the Arabian Sea: Controls on barite preservation in marine sediments. *Geochim. Cosmochim. Acta*, **65**, 1545–1556.

Schnetger, B., H.-J. Brumsack, H. Schale, J. Henrichs and L. Dittert (2000): Geochemical characteristics of deep-sea sediments from the Arabian Sea: a high resolution study. *Deep-Sea Res., Part II*, **47**, 2735–2768.

Schulte, S., F. Rostek, E. Bard, J. Rullkötter and O. Marchal (1999): Variation of oxygen minimum and primary productivity recorded in sediments of the Arabian Sea. *Earth Planet. Sci. Lett.*, **173**, 205–221.

Schulz, H., U. von Rad and H. Erlenkeuser (1998): Correlation between Arabian Sea and Greenland climate oscillations of the past 110,000 years. *Nature*, **393**, 54–57.

Shimmield, G. B. (1992): Can sediment Geochemistry record changes in coastal upwelling paleoproductivity? Evidence from Northwest Africa and the Arabian Sea. In *Upwelling Systems: Evolution since the Early Miocene*, ed. by C. P. Summerhayes, W. L. Prell and K.-C. Emis, *Geol. Soc. London Spec. Publ.*, **64**, 29–46.

Shimmield, G. B. and S. R. Mowbray (1991): The inorganic geochemical record of the northwest Arabian Sea: A history of productivity variation over the last 400 ky from site

722 and 724. *Proceedings of Ocean Drilling Program Scientific Results*, **117**, 409–429.

Shimmield, G. B., S. R. Mowbray and G. P. Weedon (1990): A 350 ka history of the Indian Southwest Monsoon.—evidence from deep-sea cores, northwest Arabian Sea. *Trans. Royal Society Edinburg: Earth Sci.*, **81**, 289–299.

Singh, A. D., D. Kroon and R. S. Ganeshram (2006): Millennial scale variations in productivity and OMZ intensity in the eastern Arabian Sea. *J. Geol. Soc. India*, **68**, 369–378.

Sinha, A., K. G. Cannariato, L. D. Stott, H.-C. Li, C.-F. You, H. Cheng, R. L. Edwards and I. B. Singh (2005): Variability of Southwest Indian summer monsoon precipitation during the Bølling-Ållerød. *Geology*, **33**, 813–816.

Sirocko, F., M. Sarnthein, H. Erlenkeuser, H. Lange, M. Arnold and J.-C. Duplessy (1993): Centuary scale events in monsoonal climate over the past 24,000 years. *Nature*, **364**, 322–324.

Sirocko, F., D. Garbe-Schonberg, A. McIntyre and B. Molino (1996): Teleconnections between the subtropical monsoons and high latitude climates during the last deglaciation. *Science*, **272**, 526–529.

Sirocko, F., D. Garbe-Schonberg and C. Devey (2000): Processes controlling trace element geochemistry of Arabian Sea sediments during the last 25,000 years. *Global Planetary Change*, **26**, 217–303.

Stuiver, M., P. J. Reimer and R. W. Reimer (2005): CALIB 5.02 (program and documentation). <http://www.calib.qua.ac.uk/>

Thamban, M., V. P. Rao and S. V. Raju (1997): Controls on organic carbon distribution in sediments from the eastern Arabian Sea margin. *Geo-Marine Lett.*, **17**, 220–227.

Thamban, M., V. P. Rao, R. R. Schneider and P. M. Grootes (2001): Glacial to Holocene fluctuations in hydrography and productivity along the southwestern continental margin of India. *Palaeogeogr. Palaeoclimat. Palaeoecol.*, **165**, 113–127.

Thomson, J., S. Nixon, I. W. Croudace, T. F. Pederson, L. Brown, G. T. Cook and A. B. Mackenzie (2001): Redox sensitive element uptake in north east Atlantic Ocean sediments (Benthic Boundary layer experimental sites). *Earth Planet. Sci. Lett.*, **184**, 535–547.

Tiwari, M., R. Ramesh, B. L. K. Somayajulu, A. J. T. Jull and G. S. Burr (2005): Early glacial (~19–17 ka) strengthening of the northeast monsoon. *Geophys. Res. Lett.*, **32**, L19712, 1–4.

Van Campo, E., J.-C. Duplessy and M. Rossignol-A Strict (1982): Climatic conditions deduced from a 150-kyr oxygen isotope-pollen record from the Arabian Sea. *Nature*, **296**, 56–59.

Van der Weijden, C. H., G. J. Reichart and H. J. Visser (1999): Enhanced preservation of organic matter in sediments deposited within the oxygen minimum zone in the northeast-ern Arabian Sea. *Deep-Sea Res., Part I*, **46**, 807–830.

Van der Weijden, C. H., G. J. Reichart and B. J. H. Vanos (2006): Sedimentary trace element records over the last 200 kyr from within and below the northern Arabian Sea oxygen mini-mum zone. *Mar. Geol.*, **231**, 69–88.

Vigliotti, L. (1997): Magnetic properties of light and dark sedi-ment layers from the Japan Sea: Diagenetic and paleoclimatic implications. *Quat. Sci. Rev.*, **16**, 1093–1114.

Vigliotti, L., L. Capotonde and M. Torh (1999): Magnetic prop-erties of sediments deposited in suboxic-anoxic environ-ments: relationships with biological and geochemical prox-ies. In *Palaeomagnetism and Diagenesis in Sediments*, ed. by D. H. Tarling and P. Turner, *Geol. Soc. London Spec. Publ.*, **151**, 71–83.

von Rad, U., H. Schulz, V. Riech, M. den Dulk, U. Berner and F. Sirocko (1999): Multiple monsoon-controlled breakdown of oxygen minimum conditions during the past 30,000 years documented in laminated sediments off Pakistan. *Palaeogeogr. Palaeoclimat. Palaeoecol.*, **152**, 129–161.

Von Stackelberg, U. (1972): Faziesverteilung in sedimenten des indisch-pakistanischen kontinentalrandes. *“Meteor” Forschungs-Ergebnisse*, C(9), 1–73.

Weedon, G. P. and G. B. Shimmield (1991): Late Pleistocene upwelling and productivity variations in the Northwest In-dian Ocean deduced from spectral analyses of geochemical data from sites 722 and 724. In *Proceedings of Ocean Drill-ing Program*, ed. by W. L. Prell and N. Niituma, *Scientific Results*, **117**, 409–429.

Zheng, Y., A. van Geen and R. P. Anderson (2000): Intensification of the northeast Pacific oxygen minimum zone during the Bölling-Ållerød warm period. *Palaeoceanography*, **15**, 528–536.